# Synchronizing Microgrid Under Different Modes of Operations

Geeta Pathak[1] · Bhim Singh[2] · B. K. Panigrahi[2]

**Abstract**  This work deals with three-phase wind energy based microgrid (WMG) having synchronization ability with the utility grid. This WMG performs multiple actions i.e. it works in isolation mode under grid abnormal conditions; operates in grid connected mode during healthy grid condition; behaves as a DSTATCOM under poor wind or no wind condition. It is capable of providing smooth transition during grid synchronization or isolation operation and effectively maintains both power balance and power quality. It resolves power quality issues i.e. voltage and current harmonics, reactive power compensation, voltage regulation etc. during steady state operations of standalone and grid tied modes. Control methods are implemented with simplicity and accuracy in voltage control and current control modes. Dual stage wind power boosting is done using a perturbation and observation technique through a boost converter. Single VSI performs backup operation and grid synchronization with reduced control complexity. It provides power quality solutions and during poor wind works like DSTATCOM. This topology is economic and simple as, diode bridge is employed in place of left side VSI of wind generation. Experimental results are presented on a laboratory prototype of WMG during all required modes of operations such as wind variations, synchronization and isolation.

## Introduction

World's dependency on electrical energy is increasing day by day. Nevertheless, corona pandemic and lockdown situation have brought about irregular supply of industry raw material and goods. Energy generation sector is also affected in terms of the delayed and insufficient supply of fossil fuels viz. mainly coal and diesel. Insufficient power generation carries significant impact on small scale industry, agriculture, rural areas and on community loads comprising both linear and nonlinear loads in nature. Based on the studies of Ministry of Power, Govt. of India, the total growth in the generation is reduced by 0.95% and -0.5% during pandemic years 2019–20 and 2020–21, respectively [1]. At present the effect of covid is still persisting in coastal states viz. Kerala, Maharashtra, Tamilnadu etc. A three phase wind based microgrid (WMG) can become a prudent choice of energy generation for smooth conduction of small industries and community loads during energy crisis situation as well as in normal situation. As it is well known that fossil fuel-based energy resources have come into the declining state due to their exhaustive utilization. As far as cost is concerned, renewable energy generation may have an edge over the fossil fuel based generation due to low cost of wind energy and implementation of advance research. Though the research concepts with renewable energy resources [2–4] and distributed generation are not new but it has been appreciated and promoted significantly from the last decade as it is based on clean and green energy, which is environment friendly and the technical advancement as well as subsidies have made its

✉ Geeta Pathak
pathakgita28@gmail.com

1   Department of Electrical Engineering, College of Technology, GBPUAT, Pantnagar, U S Nagar, Uttarakhand 263145, India

2   Department of Electrical Engineering, Indian Institute of Technology Delhi, Hauz Khas, New Delhi 110016, India

2146

J. Inst. Eng. India Ser. B (December 2022) 103(6):2145–2156

price affordable. Such systems can also sell energy by feeding excess energy to the grid. Good literature on converter topologies is being used with satisfactory performance for energy transfer among various units of MGs [5, 6].

Various control methods of VSI (Voltage Source Inverter) for the grid connected and standalone operations are explained in the literature. In the researches [7, 8], the control methods for utility interfaced systems are explained with current control approaches. In the literature [9, 10], the authors have proposed the control algorithms for isolated power generation systems. Grid synchronization concept is reported in the investigations [11] detailing about the challenges during the transition between two modes (standalone & grid tied mode) in synchronization or isolation processes. This switching may lead power imbalance among various generating units due to low inertia or poor dynamics. The battery bank is a good solution in order to meet such power imbalance. Therefore, due to controlled charging and discharging at high frequency switching, proper heat dissipation from the capacitor does not take place in time. Therefore, these systems arise high risk due to converter harmonics. Literature related to microgrid operations [7–11] provides motivation for this work where in order to make the battery system less burdened, direct attachment of it at DC link of VSI is done under proposed topology. Further battery storage can mitigate the system issues by improving the power factor of the system, regulating voltage and frequency, reducing fluctuations, standardizing the intermittency of the renewable sources; hence providing balance among generation and demand units. Angular stability is affected by low inertia systems, it may cause voltage and frequency instability. System stability and power quality problems can be resolved by applying good control algorithms for both modes of operations and using battery support during synchronization.

In this paper, the wind generator and the storage are directly attached to the DC link of VSI. Therefore, number of converters and switches are reduced in comparison to other topologies reported in the literature [12, 13]. Performance of wind based MG in standalone and grid tied operations is presented with smooth transition between these modes. In standalone mode, microgrid VSI operates in voltage control and feeds the local load demand. The battery charges and discharges depending on load demand and wind availability. During the grid recovery, the process of synchronization connects the STS (Static Transfer Switch). The control of VSI shifts from voltage control technique to current control technique. In grid connected operation, the VSI supplies excess power to the mains and at low wind generation or high load demand, the utility delivers power to local loads. The transient free connection and isolation are achieved and are demonstrated with variety of results. The main aspects of this work are briefed as follows:

- Power quality issues like voltage and frequency regulation, harmonics mitigation, power balance, etc., are taken care in all states of operation.
- MG has plug and play capability; seamless functioning with both control methods during synchronization and isolation process.
- During standalone operation, it works as a back-up system and supports local area network under grid failure. It increases reliability as well as stability aspects with this functioning.
- The battery is directly attached at the capacitor of DC bus therefore is not prone to high frequency switching during charge and discharge and has better life and less losses.
- Proposed topology is economic and simple due to reduced number of converters as, P&O (Perturb and Observe), a HIL climb method is utilized for wind MPPT and is able to reduce sensors, i.e., wind speed sensor, position sensor, and generator speed sensor to reduce the system cost. The battery and the wind energy converted into DC power using a diode rectifier are attached at the DC bus of the same VSI. Here two converters requirement is reduced and the control complexity is also minimized.

This MG concept is validated by incorporating test results on a developed porotype of three-phase WMG. Table 1 shows the overall brief of the wind power generation and Table 2 shows comparative study on various control system.

## System Structure

A permanent magnet BLDC (Brushless-DC) generator based three phase WMG is shown in Fig. 1. The wind generator is connected to a diode bridge rectifier, which converts AC power from the wind generator into DC power. After maximum power point tracking (MPPT) implementing P&O (Perturbation and observation) approach [14] using a DC-DC boost converter, it is fed to DC bus capacitor of the VSI. A battery bank support is applied at the DC bus capacitor to manage power balance during excess generation or peak demands. Using VSI with the appropriate control method, the DC power is transformed into the AC power. Three-phase nonlinear/linear loads with RC filters and interfacing inductances ($L_f$) are used at common point coupling (PCC) to reduce current harmonics and voltage harmonics. This WMG is connected or is disconnected from the grid according to its availability via STS (Static Transfer Switch). The closing and opening of STS depend on the grid condition to produce a synchronization signal. The design data of WMG are given in Table 3.

**Table 1** Main outcomes of Result and discussion section

| Operation condition | High wind power generation at less demand (Sect. 4.1) | Low wind power generation at high demand (Sect. 4.2) |
|---|---|---|
| 1. Steady state (a) Standalone | Power quality of voltages at PCC is maintained below 5% as per IEEE 519 Standard | Power quality of voltages at PCC is maintained as per IEEE 519 Standard |
| | Battery is charged as excess wind generation after supplying the local loads | 2. Battery is discharged as less wind generation to supply deficit power to the local loads |
| (b) Utility Tied | Grid currents and voltages power qualities are maintained below 5% as per IEEE 519 Standard | Grid voltages power qualities are maintained as per IEEE 519 Standard |
| | Excess wind power is fed to the utility grid after fulfilling the load demand | 2. Energy deficit between generation and the load is provided by the utility grid |
| 2. Dynamics (Sect. 4.3) | Synchronization & isolation | DSTATCOM |
| | Switching between isolation and synchronization mode is very smooth, transient free; it has no effect on PCC voltage and load currents | During poor or no wind conditions, VSI operates in DSTATCOM mode, grid voltage comes in same phase from $180^0$ phase shift (VSI operation) |
| | This synchronization and isolation processes are fast and can be observed with grid current ($i_{g\_a}$) appearance and load voltage and grid voltage angle positions ($\theta_g$ & $\theta_{sa}$) | It operates in power factor correction mode by improving grid pf to unity with load at lagging pf |
| | | Battery is in idle mode just to support the DC link therefore battery current is at zero. During this operation grid is feeding to the loads rather than fed by wind generation |

**Table 2** Indices for comparative study on various controls' behaviors

| Behavior | Controls | SOGI | LMLS | EPLL |
|---|---|---|---|---|
| Steady State | Load current THD | 23.65% | 23.65% | 23.65% |
| | Source current THD | 1.35% | 1.85% | 2.42% |
| | Voltage THD | 0.09% | 0.15% | 0.35% |
| Dynamics | Convergence rate | Fastest | Faster | slowest |
| | Complexity | low | high | average |

## Control Methods of WMG

WMG has to perform different operations as per the grid and load behavior. The three phase VSI is communicating with all the units with appropriate control method to provide satisfactory performance of WMG for the community. In standalone operation, VSI functions with VCM and in grid tied operation, it works in CCM. Both voltage and current
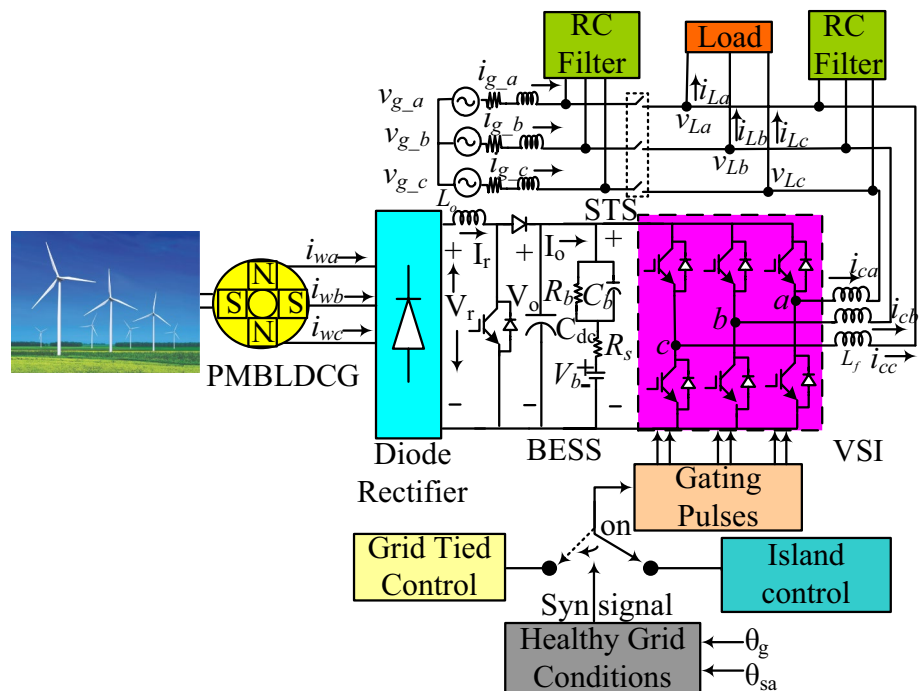
**Fig. 1** Schematic diagram of WMG

**Table 3** Microgrid components and design

| S no. | MG Component | Design calculation | Rating |
|---|---|---|---|
| 1 | 3-phase wind Generator (PMBLDC): | $P_{wind} = P_{mppt}$<br>$I_{\_w} = \frac{P_{wind}}{3V_t}$ | 3.7 kW, 13A,<br>230 V,1500 rpm |
| 2 | Battery bank: | 12 V, 7Ah: 30 series batteries | 2.520 kW |
| 3 | Input inductor of boost convertor: | $L_o = \frac{V_0}{4 \times f_{ss} \times \Delta I_L}$, $V_0 = 360$, $f_{ss} = 20$ kHz, ripple $\Delta I_L = 20\%$ | 4 m H |
| 4 | Interfacing-inductance- $L_f$: | $L_f = \left(\frac{\sqrt{3}}{2}\right) \times \frac{mV_o}{6af_s I_{rpl}}$, m = 1, a = 1.2, $f_s$ = 10 kHz, $I_{rpl}$ = 15% | 3.5 mH |
| 5 | DC link voltage $V_o$: | $V_0 = \frac{2\sqrt{2}}{\sqrt{3}m}V_L$, m = 1, $V_L$ = 220 | 360 V |
| 6 | DC-link capacitance $C_{dc}$: | $C_0 = \frac{k\{3U_{ph}(a \times i_{VSI})t\}}{0.5(V_{0max}^2 - V_{0min}^2)}$, a = 1.2, t = 350 µs, $V_{0max}$ = 360 V, $V_{0min}$ = 350 V | 1600µF |
| 7 | RC filter: | $Z = \sqrt{\left(R^2 + \left(\frac{1}{2\pi fc}\right)^2\right)}$ | R = 5Ω<br>C = 10µF |
| 8 | PI controller (standalone mode) Gains: $k_p$, $k_i$ | "—" | 3.5<br>0.3 |
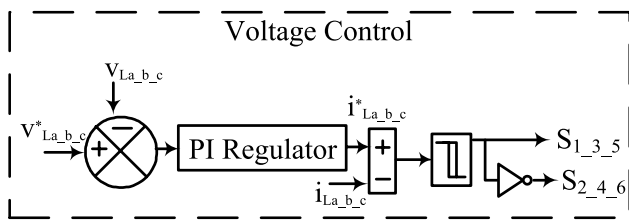


**Fig. 2** VCM for standalone operation

control methods are very simple and robust. By proper control on STS opening and re-closure the transfer between two modes, is made seamless and transient free.

## Control Method for Standalone Operation

The WMG operates in standalone operation when some abnormalities appear in the grid and system has to work in back-up mode for smooth conduction of the community load. Figure 2 demonstrates the voltage control method for PWM pulse generation of VSI. The load voltage references are formed with peak reference voltage and frequency ($V_p^*$, $\omega_0$).

The voltage references are achieved in the standalone operation as [15],

$$v_{La}^* = V_p^* \sin \omega_0 t \tag{1}$$

$$v_{Lb}^* = V_p^* \sin \left(\omega_0 t - 120^0\right) \tag{2}$$

$$v_{Lc}^* = V_p^* \sin \left(\omega_0 t + 120^0\right) \tag{3}$$

Voltage references are compared with sensed load voltages ($v_{Labc}$) and voltage errors are sent to PI regulators, to generate load current references ($i_{Labc}^*$). A comparison of sensed ($i_{Labc}$) and reference ($i_{Labc}^*$) currents, is made for pulse generation of VSI.

## Control Method for Utility tied Operation

During normal grid running conditions, Fig. 3 depicts the current control for the utility tied operation of MG to compute reference grid currents. A second order generalized integrator (SOGI) [16, 17] is implemented to extract fundamental current components from load currents. This current control is used to compute reference grid currents. The grid phase voltages ($v_{g\_abc}$) are derived [18] from grid line voltages as,

$$v_{g\_a} = \frac{1}{3}\left(2v_{g\_ab} + v_{g\_bc}\right) \tag{4}$$

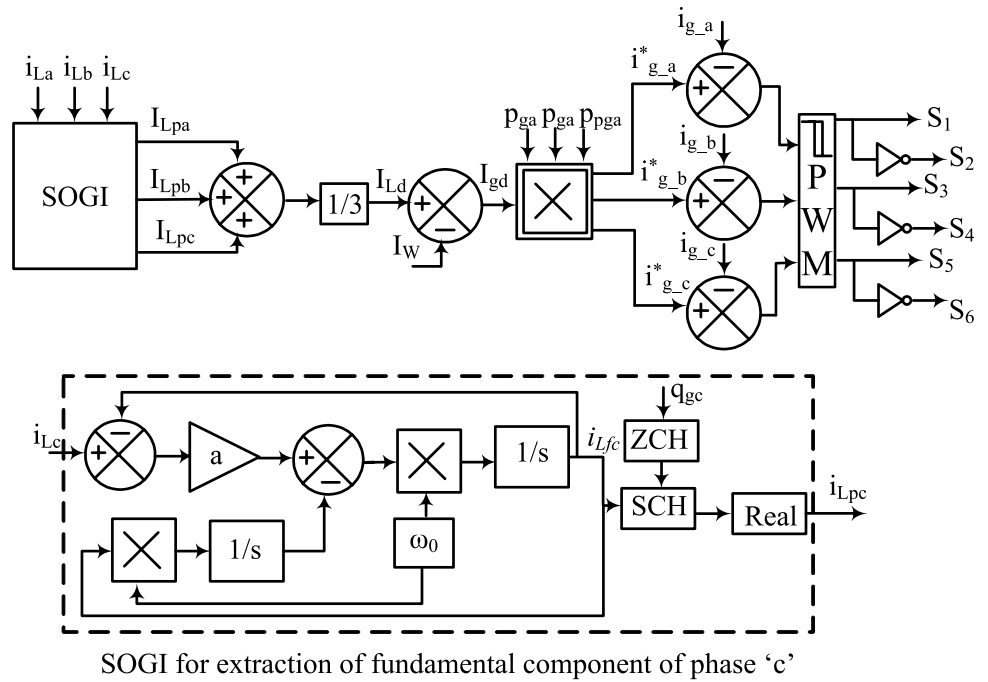$$v_{g\_b} = \frac{1}{3}\left(-v_{g\_ab} + v_{g\_bc}\right) \tag{5}$$

$$v_{g\_c} = \frac{1}{3}\left(-v_{g\_ab} - 2v_{g\_bc}\right) \tag{6}$$

The terminal voltage amplitude $V_{g\_t}$ is calculated from grid phase voltages as,

$$V_{g\_t} = \sqrt{\left(2\left(v_{g\_a}^2 + v_{g\_b}^2 + v_{g\_c}^2\right)\Big/3\right)} \tag{7}$$

where $v_{g\_a}$, $v_{g\_b}$, $v_{g\_c}$ are grid phase voltages.

**Fig. 3** An indirect current control in utility tied operation



SOGI for extraction of fundamental component of phase 'c'

The in-phase unit vectors are estimated as,

$$p_{ga} = \frac{v_{g\_a}}{V_{g\_t}}, p_{gb} = \frac{v_{g\_b}}{V_{g\_t}}, p_{gc} = \frac{v_{g\_c}}{V_{g\_t}} \qquad (8)$$

The quadrature unit vectors are obtained as,

$$q_{ga} = \frac{(p_{gc} - p_{gb})}{\sqrt{3}} \qquad (9)$$

$$q_{gb} = \frac{(3q_{ga} + q_{gb} - q_{gc})}{2\sqrt{3}} \qquad (10)$$

$$q_{gc} = \frac{(-3p_{ga} + p_{gb} - p_{gc})}{2\sqrt{3}} \qquad (11)$$

The fundamental load current component for phase 'c' ($i_{Lfc}$) is extracted using SOGI scheme. At zero crossing (ZCH) of $v_{qgc}$ with a sample and hold (SCH) logic, individual active component for phase 'c' ($i_{Lpc}$) is generated from load fundamental current $i_{Lfc}$.

An active component of the 3−φ load currents is estimated as,

$$I_{Ld} = \frac{I_{Lpa} + I_{Lpb} + I_{Lpc}}{3} \qquad (12)$$

The reference grid active current component is extracted as,

$$I_{gT} = (I_{Ld} - I_{\_w}) \qquad (13)$$

where an equivalent wind current, $I_{\_w}$ is estimated as,

$$I_{\_w} = \frac{P_{wind}}{3V_t} \qquad (14)$$

where $P_{wind} = I_r * V_r$ (input current and voltage of boost converter), $P_{bt}$ and $V_{g\_t}$ are the MPPT wind power, the battery power and the peak of terminal voltages.

Reference values of grid currents ($i^*_{g\_abc}$) are produced multiplying reference grid active current component ($I_{gd}$) with in-phase unit vectors. The VSI switching is made by comparing reference values ($i^*_{g\_abc}$) and sensed values of grid currents ($i_{g\_abc}$) to generate PWM pulses for VSI.

**Grid and Load Angles Estimation and Load Angle Correction**

The grid and load voltages angles ($\theta_g$, $\theta_{sa}$) are generated using three phase PLL (Phase Lock Loop). Angle error signal is send to the PI regulator. The PI regulator
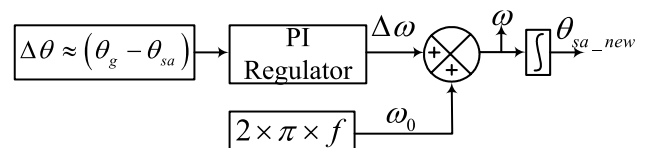


**Fig. 4** Control of an angle of load voltage close to grid voltage angle

2150

J. Inst. Eng. India Ser. B (December 2022) 103(6):2145–2156

regulates the frequency difference (Δω) as depicted in Fig. 4. The change is incorporated in load voltage angle ($\theta_{sa}$) for updating it close to an angle of the grid voltage ($\theta_g$).

## WMG Responses

Steady state performance of WMG is observed at nonlinear loads with wind speed variations. Two scenarios are considered as: (1) high wind power generation at low load demand, and (2) low wind power generation at high load demand. Dynamic behavior is studied at linear/nonlinear loads. The voltages and currents at common coupling points (PCC) are detected using Hall Effect voltage and current sensors. The control methods are applied on a DSP-dSPACE 1103. An Agilent make- DSO-7014A, DSO (Digital Storage Oscilloscope) and Fluke-43B, a power analyzer are employed to record results.

### Condition1: High Wind power Generation at Less Demand

At reduced load demand with full capacity wind power generation, the excess power is delivered to the grid during utility tied operation and is put into the battery storage during standalone operation.

*Standalone Operation*

The steady state functioning of WMG for the standalone operation is taken with voltage control method as revealed in Fig. 5. The load current ($i_{Lc}$) at line voltage ($v_{Lab}$), their THDs are shown in Fig. 5a, b. The VSI current ($i_{VSI\_c}$) and the load voltage THDs are illustrated in Fig. 5c, d. The load voltage is sinusoidal and its harmonics content is very small. This justifies that WMG control is effective in improving voltage profile under standalone operation. Figure 5e, f depicts that VSI power satisfies the load demand. The wind generation is higher than the demand as shown in Fig. 5g, h. So, the rest power is conserved in the battery. A part of power is consumed in system losses.

*Utility Tied Operation*

The WMG behavior in utility tied operation is demonstrated in Fig. 6. The VSI is operating in current control mode. Figure 6a, b shows the line voltage and grid current ($i_{gc}$) with its THD. The voltage THD is shown in Fig. 6c. The current control algorithm is capable of improving the power quality. Figure 6d–f illustrates the load currents ($i_{Lc}$), its THD and VSI current ($i_{VSI\_c}$). The wind power generation is revealed in Fig. 6g. The VSI power ($P_{VSI}$), grid power ($P_g$) and demand ($P_L$) are shown in Fig. 6h–j. The renewable power is fed to the load and the grid (negative in sign) through VSI. The battery power ($P_{bt}$) shown in Fig. 6k is negative, which shows that the battery releases power for system losses.
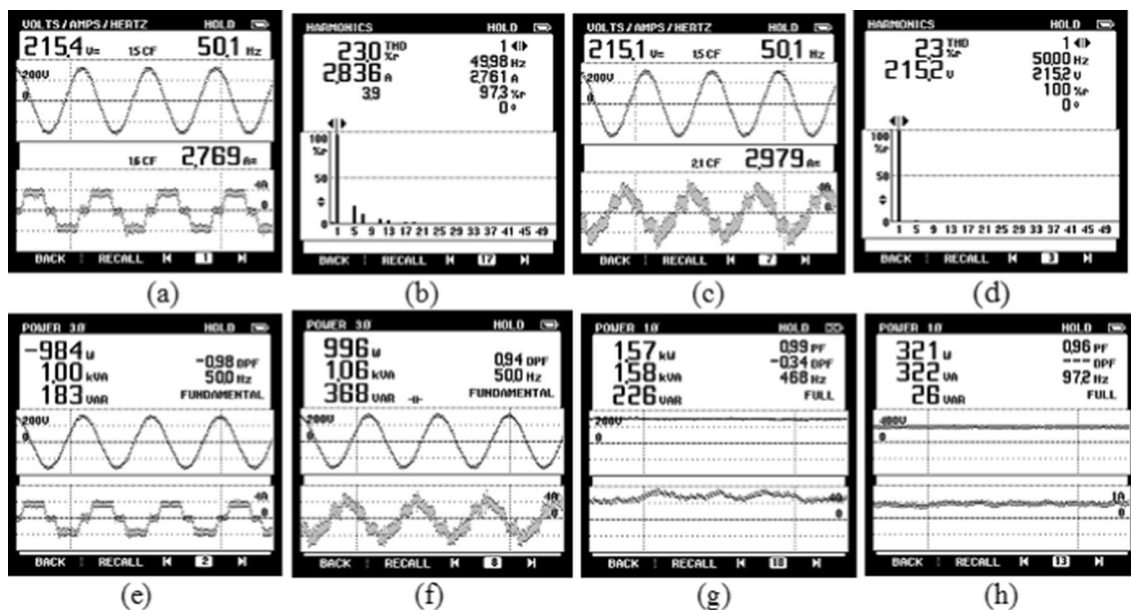


**Fig. 5** **a** Load currents (iLc) with VLab **b** Load current THD **c** Current of VSI (iVSI_c) with VLab **d** THD of load voltage **e** PL **f** PVSI **g** P_w **h** Pbt
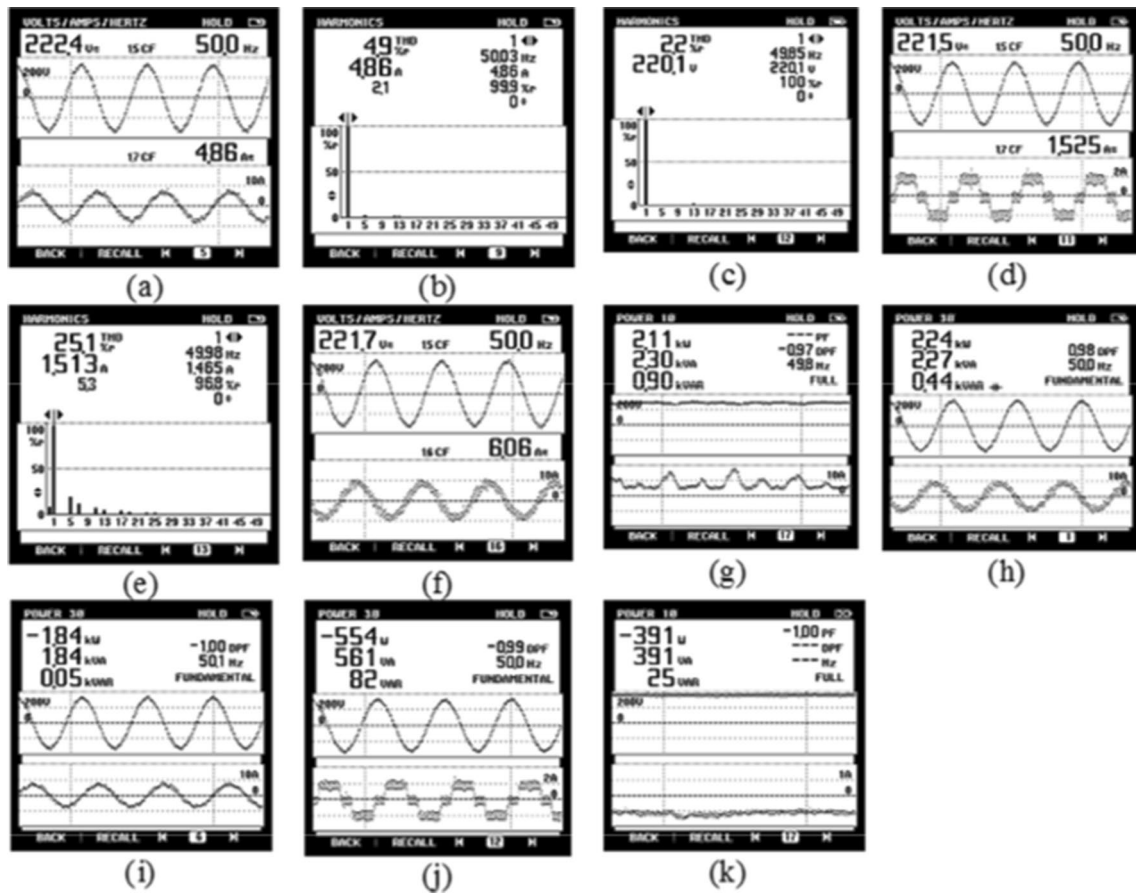
**Fig. 6** **a** Utility-grid currents (iug_c) with vg_ab **b** THD of grid current **c** THD of line voltage **d** Load currents (iLc) with Vg_ab **e** THD of load current **f** VSI currents (iVSI_c) with Vg_ab **g** P_w **h** PVSI **i** Pg **j** Load demand (PL) **k** Battery power (Pbt)

## Condition 2: Low Wind Power Generation at High Demand

With low wind power generation, the extra load demand is fulfilled by the battery storage during standalone condition. At grid availability and grid connected operation, the power is supplied by the mains.

### *Standalone Operation*

Figure 7 demonstrates the steady state scenario of the WMG in a standalone operation when it realizes high load demand. Figure 7a, b depicts the load current and load voltage THD. Figure 7c–f illustrates different power states during high load demand. It is shown that VSI ($P_{VSI}$) is supplying the sufficient power to the load ($P_L$). The wind generation ($P_w$) is not sufficient to fulfill the load demand shown in Fig. 7e, therefore, the battery discharges to provide rest of the required power ($P_{bt}$) as depicted in Fig. 7f.

### *Utility Tied Operation*

With grid availability and low wind speeds having less power generation, the grid supplies deficit power to the load. This detailed scenario in utility tied state is shown in Fig. 8. Figure 8a–c presents utility current (ig_c), load current (iLc) and VSI current (iVSI_c).

The whole energy scenario is shown in Fig. 7d–h. The load demand ($P_L = 1.69$ kW) is much higher than the wind power ($P_w = 183$ W). Therefore, as VSI is providing very small power to the load ($P_{VSI}$), the rest power is coming from the grid ($P_g = 1.58$ kW). VSI power and battery powers are shown in Fig. 7g, h, respectively.

It is observed that during steady state operation, the WMG control methods are effective to provide power balance as well as power quality.
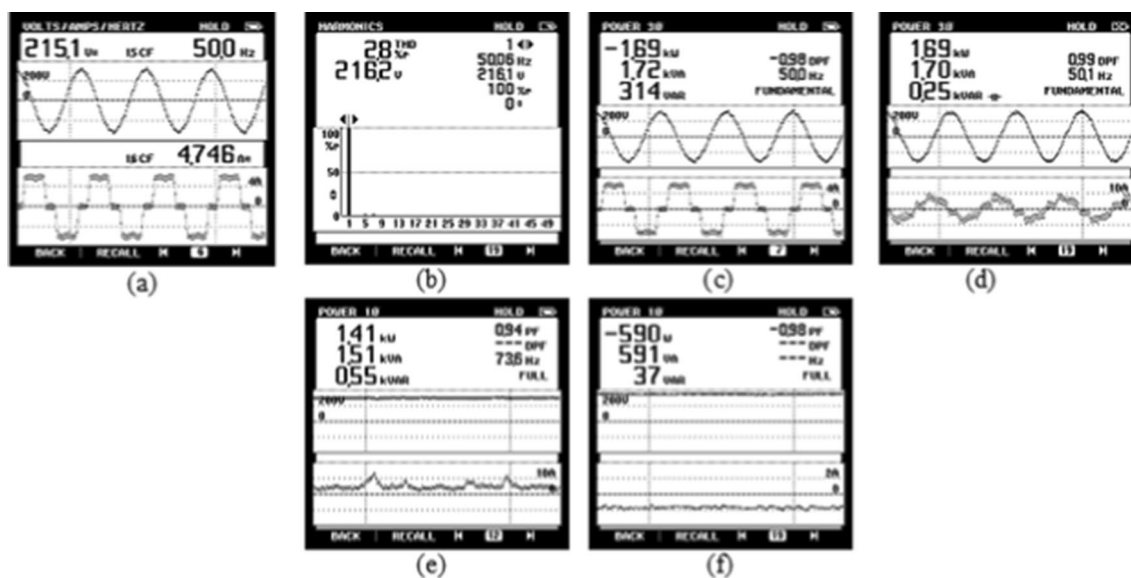
2152

J. Inst. Eng. India Ser. B (December 2022) 103(6):2145–2156



**Fig. 7** **a** Load current (iLc) **b** THD of line voltage **c** Load demand (PL) **d** PVSI **e** Wind power (Pw) **f** Battery power (Pbt)
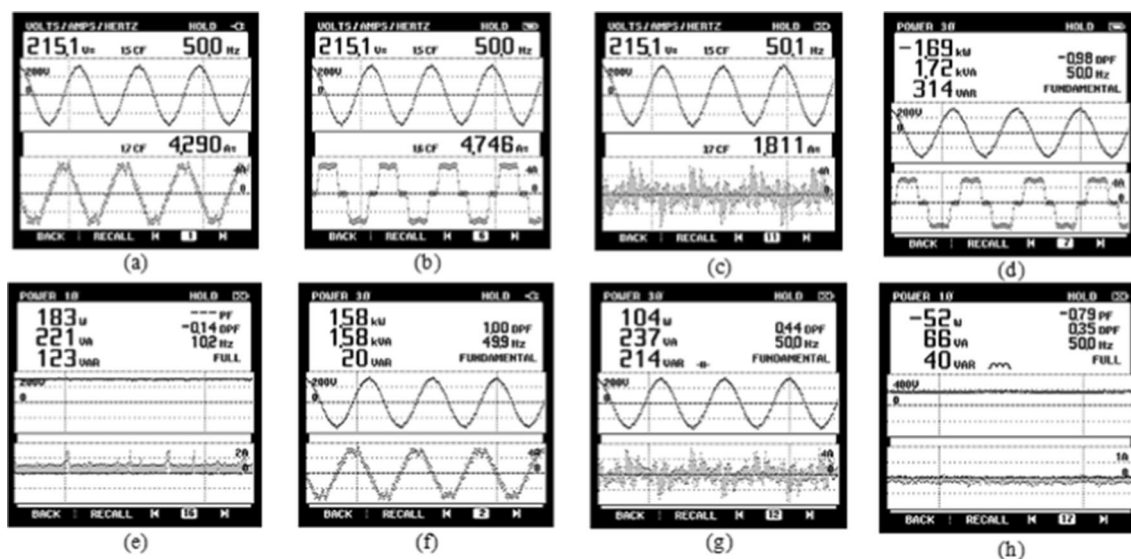


**Fig. 8** **a** Utility-grid current (ig_c) **b** Load current (iLc) **c** Currents of VSI (iVSI_c) **d** Load demand (PL) **e** P_w **f** Pg **g** PVSI (h) Battery power (Pbt)

## Dynamics Under Synchronization, Isolation and DSTATCOM Operations

The dynamic performance of WMG is achieved experimentally at linear/nonlinear loads synchronizing grid, grid isolation and DSTATCOM operation with wind speeds variation. The WMG is functioning in standalone operation to feed the community loads and it synchronizes to the grid as per IEEE 1547 [19] and delivers power to the grid as soon as it comes back to the healthy state. Figure 9 illustrates various signals of synchronizing grid and

isolation operations. Figure 9a shows both isolation and synchronization together. During the isolation, the grid line voltage ($v_{g\_ab}$) and current ($i_{g\_a}$) both disappear instantaneously without having spikes in load voltage ($v_{Lab}$) and current ($i_{La}$). The synchronization takes place within few cycles after the grid voltage appearance and the grid current $i_{g\_a}$ comes into the picture. The load line voltage ($v_{Lab}$) and current ($i_{La}$) are maintained constant without spikes. Figure 9b, c illustrates the grid current ($i_{g\_a}$) with grid and load angles ($\theta_g$ & $\theta_{sa}$) at grid synchronization and isolation under nonlinear loads. The smooth transfer between the
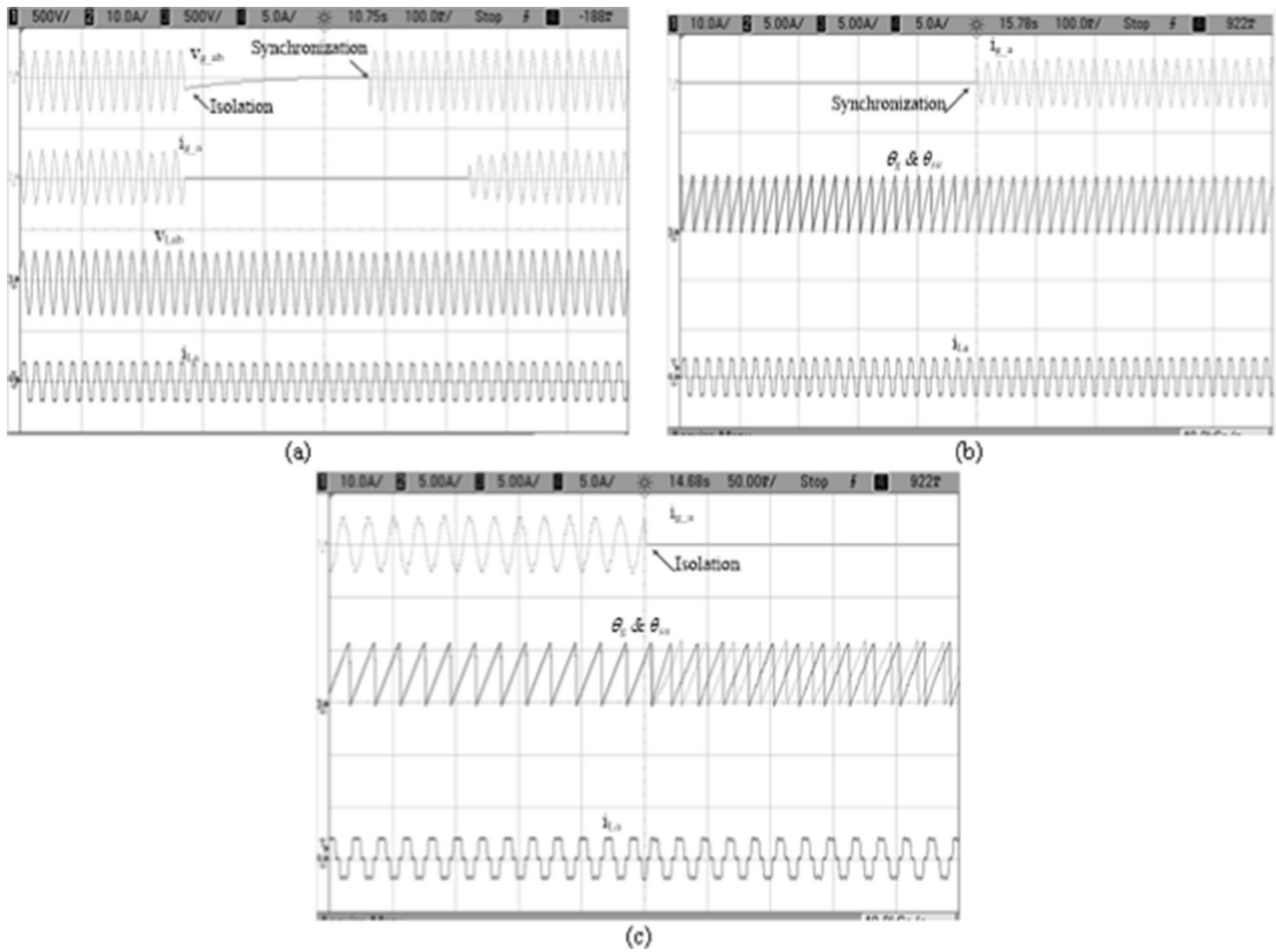
**Fig. 9** Dynamics of WMG under nonlinear loads **a** vg_ab, ig_a, vLab, iLa **b–c** ig_a, θg, θsa, iLa

modes is achieved using the appropriate control methods, i.e., voltage control and current control modes.

During the grid tied operation, the WMG feeds the consumer load and the excess power is delivered to the grid. At high speed winds, the surplus wind power is fed to the utility (under $SS_1$). During low wind availability, the generation is almost reduced to zero or insufficient to feed the consumer loads as depicted in Fig. 10a. Under these circumstances, the VSI behaves as DSTATCOM ($SS_2$) and the power flows from the grid to the load. The grid currents now change with $180^0$ phase shift and in-phase with the grid voltage. Figure 10b reveals the DSTATCOM (under $SS_2$) action with linear load, where at no wind condition the grid supplies power to the load at unity power factor while the load is at lagging power factor. Therefore, reactive power compensation and power factor correction are provided by the VSI under DSTAT-COM operation. Figure 10c shows the DC bus voltage ($V_{DC}$), battery current ($I_{bt}$), wind speed variation in terms of the boost converter input current ($I_r$) and the boost

converter input voltage ($V_r$). In absence of wind power, the grid feeds power to the consumer load. Moreover, the battery either discharges or may charge or in floating state according to its state of charge. Internal parameters of wind current component ($I_r$), load active component ($I_{Ld}$), and reference grid current active component to feed grid ($I_{gd}$) and reference grid current ($i^*_{g\_a}$) are shown in Fig. 10d. $I_{Ld}$ is constant with fixed load demand. The active power component of wind current ($I_{-w}$) is changed from negative to positive with wind speed reduction, which shows that the grid is feeding the load rather than fed by the WMG. The phase of reference grid current ($i^*_{g\_a}$) also changes, which shows its action is changed now.

A comparative analysis for system dynamics is done with SOGI (second order generalized integrator), LMLS (Least Mean Logarithmic Square) in [20] and EPLL (Enhanced Phase Lock Loop) [21]. Using MATLAB Simulink, the load removal is realized in Fig. 11, on phase 'a' at t = 2.5 s and it is again revived at t = 2.7 s. During observation, the SOGI
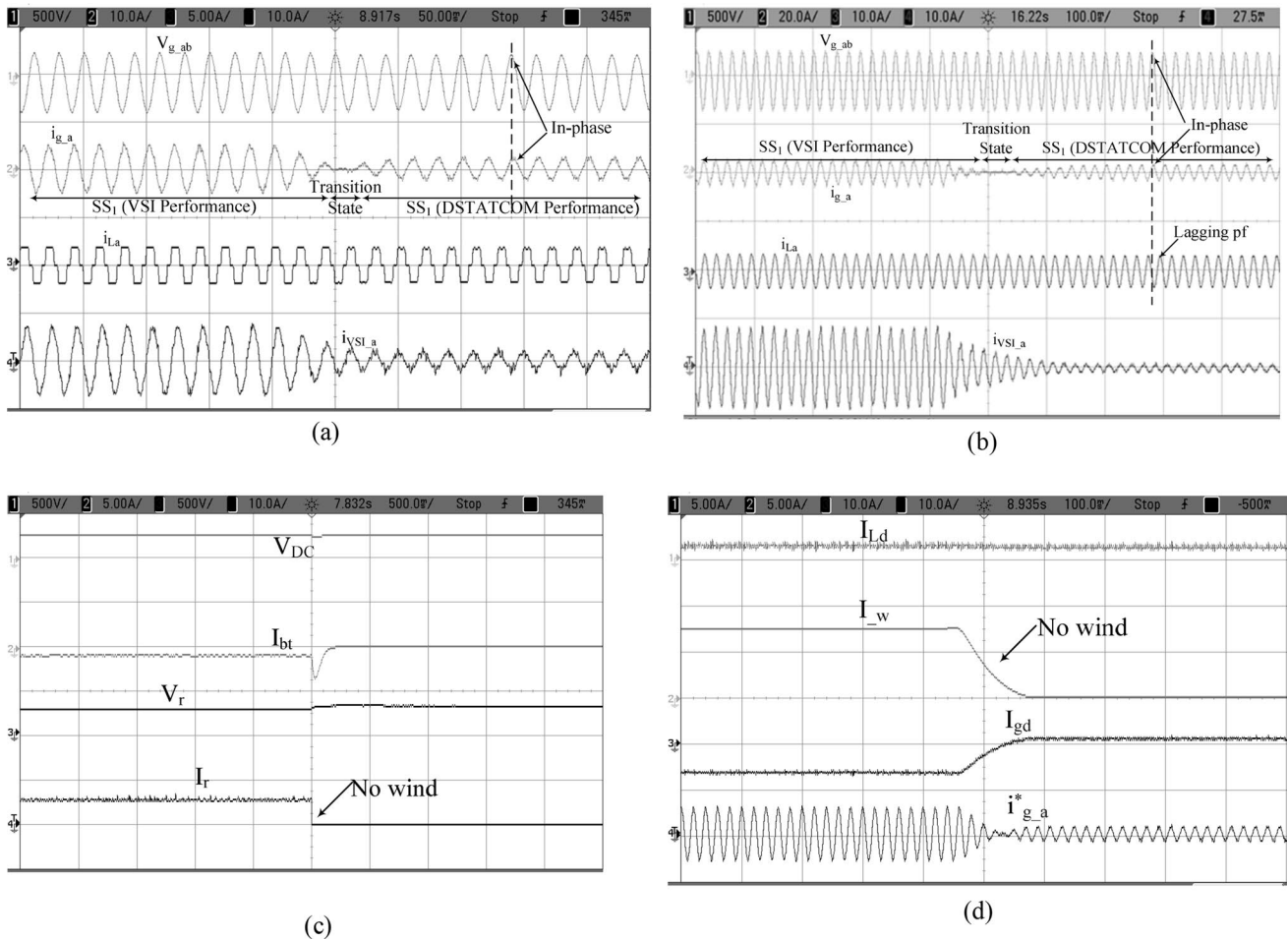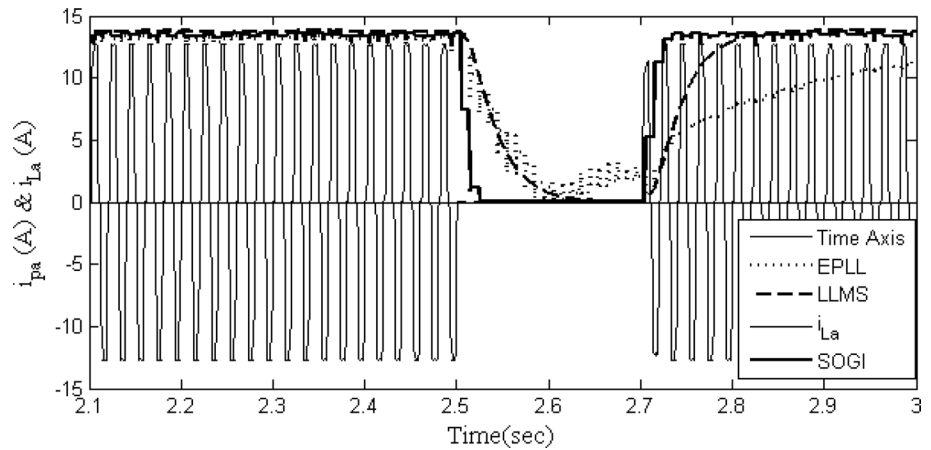
(a)



(b)



(c)



(d)

**Fig. 10** WMG dynamics with variation in wind speed **a** $v_{g\_ab}$, $i_{g\_a}$, $i_{La}$, $i_{VSI\_a}$ **b** $v_{g\_ab}$, $i_{g\_a}$, $i_{La}$, $i_{VSI\_a}$ **c** $V_{DC}$, $I_{bt}$, $V_r$, $I_r$ **d** $I_{Ld}$, $I_{\_w}$, $I_{gd}$, $i^*_{g\_a}$

**Fig. 11** Dynamic behavior of different controls



is found fastest among all the control schemes. FFT analysis for steady state operation is also done. Finally, a comparative study is included in Table 2.

**Conclusion**

A permanent magnet BLDC generator based three phase WMG prototype has been designed and developed into the laboratory to validate its performance with test results.

Performance of WMG has been demonstrated in standalone, and utility tied operations with low and high wind variations. The transient free transition between grid synchronization and isolation process has also been demonstrated effectively. The VSI has operated in voltage and current control modes seamlessly using simple and robust control methods. The synchronization control is used for switching of STS. The control methods are able to resolve power quality issues like voltage and current harmonics, voltage regulation during dynamics as mode changes from grid tied to standalone and vice-versa, and also during power reversal of the grid at low wind generation when VSI starts behaving as DSTATCOM. During standalone operation, it supports the local system as a back-up during grid failure and also increases reliability and stability of the network. VSI manages power among different units such as energy sources, battery bank and various industrial and agricultural loads in all operations. The efficient power flow, PQ and power balance are achieved under this scheme.

**Declarations**

**Conflict of interest**　None of the co-authors have a conflict of interest to disclose.

# References

1. https://powermin.gov.in/en/content/power-sector-glance-all-india.
2. G. Zhang, S. Zhang, W. Zhang, Z. Shen and L. Wang, Distributed energy management for multiple data centers with renewable resources and energy storages. IEEE Transactions on Cloud Computing, Early Access. doi: https://doi.org/10.1109/TCC.2020.3031881
3. J. Valinejad, M. Marzband, M. Korkali, Y. Xu, A.S. Al-Sumaiti, Coalition formation of microgrids with distributed energy resources and energy storage in energy market. J. Modern Power Syst. Clean Energy **8**(5), 906–918 (2020). https://doi.org/10.35833/MPCE.2019.000116
4. B. Nouri, L. Kocewiak, S. Shah, P. Koralewicz, V. Gevorgian, P. Srensen, Generic multi-frequency modelling of converter-connected renewable energy generators considering frequency and sequence couplings. IEEE Trans. Energy Convers. **37**(1), 547–559 (2022). https://doi.org/10.1109/TEC.2021.3101041
5. B. Nun, M.F. Umar, A. Karaki, M.B. Shadmand, S. Bayhan, H. Abu-Rub, Rank-based predictive control for community microgrids with dynamic topology and multiple points of common coupling. IEEE J. Emerg. Select. Topics Ind. Electron. **3**(1), 144–155 (2022). https://doi.org/10.1109/JESTIE.2021.3110746
6. A. Vettuparambil, K. Chatterjee, B.G. Fernandes, A Modular multiport converter to integrate multiple solar photo-voltaic PV modules with a battery storage system and a DC microgrid. IEEE Trans. Industr. Electron. **69**(5), 4869–4878 (2022). https://doi.org/10.1109/TIE.2021.3082063
7. M.E. Zarei, D. Ramirez, M. Prodanovic, G. Venkataramanan, Multivector model predictive power control for grid connected converters in renewable power plants. IEEE J. Emerg. Select. Topics Power Electron. **10**(2), 1466–1478 (2022). https://doi.org/10.1109/JESTPE.2021.3077953
8. Y. Khayat, S. Golestan, J.M. Guerrero, J.C. Vasquez, H. Bevrani, DC-Link voltage control aided for the inertial support during severe faults in weak grids. IEEE J. Emerg. Select. Topics Power Electron. **9**(6), 7296–7305 (2021). https://doi.org/10.1109/JESTPE.2020.3033657
9. G. Pathak, B. Singh, B.K. Panigrahi, Wind hydro microgrid and its control for rural energy system. IEEE Trans. Ind. Appl. **55**(3), 3037–3045 (2019). https://doi.org/10.1109/TIA.2019.2897659
10. G. Pathak, B. Singh, B.K. Panigrahi, Control of wind-solar microgrid for rural electrification. In Proceedings of IEEE 7th Power India International Conference (PIICON), Bikaner, India. 2016; pp. 1–5. doi:https://doi.org/10.1109/POWERI.2016.8077263
11. S. Choudhary, A comprehensive review on issues, investigations, control and protection trends, technical challenges and future directions for microgrid techniques. Int. Trans. Electr. Energy Syst. (2020). https://doi.org/10.1002/2050-7038.12446
12. Y. Cao, Y. Hu, R. Hu, J. Chen, Research on the synchronization control strategy for microgrid-connected voltage source inverter. IEEE 6th International Symposium on Power Electronics for Distributed Generation Systems (PEDG), 2015; Aachen, pp. 1–5. doi:https://doi.org/10.1109/PEDG.2015.7223062
13. M. Fatu, F. Blaabjerg, I. Boldea, Grid to standalone transition motion-sensorless dual-inverter control of PMSG with asymmetrical grid voltage sags and harmonics filtering. IEEE Trans. Power Electron. **29**(7), 3463–3472 (2014). https://doi.org/10.1109/TPEL.2013.2279883
14. Y. Xia, K.H. Ahmed, B.W. Williams, Wind turbine power coefficient analysis of a new maximum power point tracking technique. IEEE Trans. Ind. Electron. **60**(3), 1122–1132 (2012). https://doi.org/10.1109/TIE.2012.2206332
15. S. A. O. da Silva, R. A. Modesto, R. Barriviera, M. Kaster, A line-interactive UPS system operating with sinusoidal voltage and current references obtained from a self-tuning filter. IECON 2012 - 38th Annual Conference on IEEE Industrial Electronics Society, 2012; pp. 74–79. doi: https://doi.org/10.1109/IECON.2012.6388827
16. S. Golestan, J.M. Guerrero, J.C. Vasquez, A.M. Abusorrah, Y. Al-Turki, Harmonic linearization and investigation of three-phase parallel-structured signal decomposition algorithms in grid-connected applications. IEEE Trans. Power Electron. (2021). https://doi.org/10.1109/TPEL.2020.3021723
17. S. Golestan, J.M. Guerrero, J.C. Vasquez, A.M. Abusorrah, Y. Al-Turki, Standard SOGI-FLL and Its close variants precise modeling in LTP framework and determining stability region/robustness metrics. IEEE Trans. Power Electron. **36**(1), 409–422 (2021). https://doi.org/10.1109/TPEL.2020.2997603
18. G. Pathak, B. Singh, B.K. Panigrahi, A. Chandra, K. Al-Haddad, Wind-PV based microgrid and its synchronization with utility grid. IEEE International Conference on Power Electronics, Drives and Energy Systems (PEDES), pp. 1–6 (2016). doi: https://doi.org/10.1109/PEDES.2016.7914334
19. IEE Application Guide for IEEE Std 1547(TM), IEEE Standard for Interconnecting Distributed Resources with Electric Power Systems. IEEE Std 1547.2-2008, 2009: 1–217.
20. G. Pathak, B. Singh, B.K. Panigrahi, Logarithmic cost based adaptive control for wind-diesel microgrid. Annual IEEE India Conference (INDICON). 2015; 1–6. doi: https://doi.org/10.1109/INDICON.2015.7443161
21. G. Pathak, B. Singh, B.K. Panigrahi, Isolated microgrid employing PMBLDCG for wind power generation and synchronous reluctance generator for DG system. IEEE 6th India International

Conference on Power Electronics (IICPE). 2014; 1–6. doi: https://doi.org/10.1109/INDICON.2015.7443161